A PHYSICAL STRING MODEL WITH ADJUSTABLE BOUNDARY CONDITIONS

Maximilian Schäfer

Friedrich-Alexander Universität
Erlangen-Nürnberg (FAU)
Multimedia Communications
and Signal Processing
Cauerstr. 7, D-91058 Erlangen, Germany
max.schaefer@fau.de

Petr Frenštátský

Brno University of Technology
Faculty of Electrical Engineering and
Communication
Technická 3058/10, 616 00 Brno,
Czech Republic
petr.frenstatsky@
phd.feec.vutbr.cz

Rudolf Rabenstein

Friedrich-Alexander Universität
Erlangen-Nürnberg (FAU)
Multimedia Communications
and Signal Processing
Cauerstr. 7, D-91058 Erlangen, Germany
rudolf.rabenstein@fau.de

ABSTRACT

The vibration of strings in musical instruments depends not only on their geometry and material but also on their fixing at the ends of the string. In physical terms it is described by impedance boundary conditions. This contribution presents a functional transformation model for a vibrating string which is coupled to an external boundary circuit. Delay-free loops in the synthesis algorithm are avoided by a state-space formulation. The value of the boundary impedance can be adjusted without altering the core synthesis algorithm.

1. INTRODUCTION

The vibrations of strings, bars and other sound generating objects in musical instruments are a well studied subject. Based on the fundamental laws of elasticity, their dynamic behavior is accurately described by differential equations of different kinds.

There is a variety of methods to turn these differential equations into computational models by discretization in time and space or by transformation into the respective frequency domains. The procedure of deriving a real-time algorithm from a physical description of parts of a musical instrument is called physical modeling sound synthesis.

The dynamics of a vibrating body depend not only on properties like shape and material but also on the contact conditions to other parts of the musical instrument or the hands of the musician. These are relatively easy to model if the ends of a string are fixed by frets or bridges or if the ends of a bar in a xylophone are free from external forces.

Other types of contact conditions need more careful consideration. The touch and the movement of the musicians fingers can be modelled only approximately with mathematical equations. The interaction between the strings, the bridge, and the body of a musical instrument requires careful measurement of parameters like body resonances and bridge impedances. Since there is an abundance of research in this field, only a few books and overview articles with extensive references can be addressed here.

The corresponding boundary conditions are described in [1, Chap. 2.12] by conditions for the deflection (fixed end) or its first order space derivative (free end) or by complex impedances at the boundaries. Also [2, Chap. 6.1.9] discusses not only the simple cases of fixed and free ends but also lossy boundary conditions. In finite difference models, the boundary conditions are often formulated after spatial discretization by involving virtual spatial sample points beyond the boundary [2, 3]. Waveguide methods model the influence of the boundary on the reflection of waves by reflection factors or reflection filters (bridge filters) [3, 4]. The string-bridge interaction is described by a mechanical impedance (admittance) in [5].

A particular physical modeling technique is the functional transformation method [6]. It is based on the spatial eigenfunctions of vibrating bodies, which are most easily determined for fixed and for free ends. However [7] discusses also impedance boundary conditions for frequency independent impedances. The more involved case of frequency dependent impedances (typically bridge impedances) is discussed in [8] by incorporating the boundary impedance into the synthesis algorithm.

A conceptually simpler approach has been presented in general terms in [9]. There the synthesis algorithm is kept separate from the boundary model. This way, the impedance in the boundary model can be adjusted during operation without affecting the structure of the string model. The approach is motivated by the plant-controller loop familiar from control theory.

How these adjustable boundary conditions can be applied to a functional transformation model of a string is shown here in detail. Sec. 2 presents the physical model of a string and the spatial transformation is reviewed in Sec. 3. Boundary conditions are discussed in Sec. 4 with the impedance as an adjustable parameter. The occurrence of delay-free loops can be avoided by a state space approach in Sec. 5. Examples show the effect of the resulting synthesis algorithm in Sec. 6. Although the results shown here involve a frequency independent impedance, the state space approach can be extended also to frequency dependent impedances as discussed in Sec. 7.

2. PHYSICAL MODEL OF A STRING

This section describes the physical foundations of a single vibrating string. The partial differential equation describing the oscillation of a string is reformulated to serve as a starting point for the following Functional-Transformation method (FTM). The presentation is an abridged and modified version of the approach described in [10].

2.1. Physical Description

The starting point for a computational model is the partial differential equation (PDE) of a single vibrating string [10, 11]. The deflection $y = y(x, t)$ depends on the position on the string x and time t, $\dot{y}$ represents the time- and y' the space-derivative. Then the PDE of a single vibrating string is given as

$$\rho A\ddot{y} + EIy'''' - T_\mathrm{s}y'' + d_1\dot{y} - d_3\dot{y}'' = f_\mathrm{e}, \qquad (1)$$

with the cross-section area A, moment of inertia I and the length l. The material is characterized by the density ρ and Young's modulus E. T_s describes the tension and d_1 and d_3 are non-frequency and frequency dependent damping [11]. The excitation function is defined as $f_\mathrm{e} = f_\mathrm{e}(x,t)$.

The PDE (1) is reformulated into a vectorized form for subsequent transformations

$$\left[\boldsymbol{C}\frac{\partial}{\partial t} - L\right]\boldsymbol{y}(x,t) = \boldsymbol{f}_\mathrm{e}(x,t), \tag{2}$$

with the differential operator

$$L = \boldsymbol{A} + \boldsymbol{I}\frac{\partial}{\partial x} \tag{3}$$

and the vector of variables

$$\boldsymbol{y}(x,t) = \begin{bmatrix} \dot{y} & y' & y'' & y''' \end{bmatrix}^\mathrm{T}. \tag{4}$$

The system matrices of Eq. (2) are

$$\boldsymbol{C} = \begin{bmatrix} 0 & 1 & 0 & 0 \\ 0 & 0 & 0 & 0 \\ 0 & 0 & 0 & 0 \\ c_1 & 0 & c_2 & 0 \end{bmatrix} \quad \boldsymbol{A} = \begin{bmatrix} 0 & 0 & 0 & 0 \\ 0 & 0 & -1 & 0 \\ 0 & 0 & 0 & -1 \\ a_1 & 0 & a_2 & 0 \end{bmatrix} \tag{5}$$

with the coefficients

$$a_1 = \frac{d_1}{EI} \quad a_2 = -\frac{T_\mathrm{s}}{EI} \quad c_1 = -\frac{\rho A}{EI} \quad c_2 = \frac{d_3}{EI}. \tag{6}$$

The equivalence between the scalar and the vector representation follows by converting (2) back to the scalar form (1).

2.2. Boundary Conditions

The behavior of a vibrating string depends also on a set of boundary conditions in addition to the PDE (1). They can be described using a boundary matrix $\boldsymbol{F}_\mathrm{b}^\mathrm{H}$, which transforms the vector of variables $\boldsymbol{y}(x,t)$ into a vector of boundary excitations $\boldsymbol{\phi}(x,t)$

$$\boldsymbol{F}_\mathrm{b}^\mathrm{H}\boldsymbol{y}(x,t) = \boldsymbol{\phi}(x,t) \qquad x = 0, l. \tag{7}$$

The superscript H denotes the hermitian matrix. In a first simple case it is assumed, that there are unknown boundary excitations ϕ for deflection and bending moment at the boundaries of the string

$$y(x,t) = \phi_1(x,t) \qquad x = 0, l, \tag{8}$$

$$y''(x,t) = \phi_3(x,t) \qquad x = 0, l. \tag{9}$$

Since the vector of variables in Eq. (4) contains the first time derivative, Eq. (8) is turned into $\dot{y}(x,t) = \dot{\phi}_1(x,t)$ by time differentiation, such that

$$\boldsymbol{F}_\mathrm{b}^\mathrm{H} = \begin{bmatrix} 1 & 0 & 0 & 0 \\ 0 & 0 & 0 & 0 \\ 0 & 0 & 1 & 0 \\ 0 & 0 & 0 & 0 \end{bmatrix}, \quad \boldsymbol{\phi}(x,t) = \begin{bmatrix} \dot{\phi}_1(x,t) \\ 0 \\ \phi_3(x,t) \\ 0 \end{bmatrix}. \tag{10}$$

2.3. Laplace Transformation

For the following transformation of the string model a Laplace transformation has to be applied to the vectorized PDE (2) and to the boundary conditions (7), which leads to

$$\left[s\boldsymbol{C} - L\right]\boldsymbol{Y}(x,s) = \boldsymbol{F}_\mathrm{e}(x,s) \tag{11}$$

$$\boldsymbol{F}_\mathrm{b}^\mathrm{H}\boldsymbol{Y}(x,s) = \boldsymbol{\Phi}(x,s). \tag{12}$$

The complex frequency variable is s and the Laplace transforms of the time variables are denoted by uppercase letters. This model is used for the further derivations of the FTM.

3. TRANSFORMATION OF THE STRING MODEL

In this section the FTM is applied to the string model. The foundations of the transformation are described in [6, 10]. Therefore, some of the derivations regarding the transformation are skipped in the following.

3.1. Sturm-Liouville Transformation

The first step is the definition of a forward and inverse Sturm-Liouville Transformation (SLT). The forward transformation is defined as [10]

$$\mathcal{T}\left\{\boldsymbol{Y}(x,s)\right\} = \bar{Y}(\mu,s) = \int_0^l \tilde{\boldsymbol{K}}^\mathrm{H}(x,\mu)\boldsymbol{C}\boldsymbol{Y}(x,s)\mathrm{d}x, \tag{13}$$

and the inverse transformation can be written in terms of a sum as

$$\mathcal{T}^{-1}\left\{\bar{Y}(\mu,s)\right\} = \boldsymbol{Y}(x,s) = \sum_\mu \frac{1}{N_\mu}\bar{Y}(\mu,s)\boldsymbol{K}(x,\mu), \tag{14}$$

with the scaling factor

$$N_\mu = \int_0^l \tilde{\boldsymbol{K}}^\mathrm{H}(x,\mu)\boldsymbol{C}\boldsymbol{K}(x,\mu)\mathrm{d}x. \tag{15}$$

The vectors $\boldsymbol{K}(x,\mu)$ and $\tilde{\boldsymbol{K}}(x,\mu)$ are the kernel functions (eigenfunctions) of the transformation, which depend on the problem. The kernel functions fulfill different properties which are shown in [10]. The eigenfunctions $\tilde{\boldsymbol{K}}(x,\mu)$ are adjoint to the primal eigenfunctions $\boldsymbol{K}(x,\mu)$. Additionally, the two sets of eigenfunctions are biorthogonal. The integer index μ can be regarded as a discrete spatial frequency variable.

3.2. Application to the PDE

The transformation from Eq. (13) is now applied to Eq. (11). The properties of the eigenfunctions from Sec. 3.3 lead to the result

$$s\bar{Y}(\mu,s) - s_\mu\bar{Y}(\mu,s) - \bar{\Phi}(\mu,s) = \bar{F}_\mathrm{e}(x,s), \tag{16}$$

with the transformed boundary and excitation term

$$\bar{\Phi}(\mu,s) = \left[\tilde{\boldsymbol{K}}^\mathrm{H}(x,\mu)\boldsymbol{\Phi}(x,s)\right]\Big|_0^l \qquad x = 0, l, \tag{17}$$

$$\bar{F}_\mathrm{e}(\mu,s) = \int_0^l \tilde{\boldsymbol{K}}^\mathrm{H}(x,\mu)\boldsymbol{F}_\mathrm{e}(x,s)\mathrm{d}x, \tag{18}$$

where the values s_μ represent the spatial eigenfrequencies. Solving Eq. (16) for the transformed output signal gives

$$\bar{Y}(\mu,s) = \frac{1}{s - s_\mu}\left[\bar{\Phi}(\mu,s) + \bar{F}_\mathrm{e}(\mu,s)\right]. \tag{19}$$

3.3. Eigenvalue Problems

The two kernel functions of the forward and inverse SLT have to fulfill their eigenvalue problems and boundary conditions, so that the transformation is applicable in Eq. (16)

$$L\boldsymbol{K}(x,\mu) = s_\mu\boldsymbol{C}\boldsymbol{K}(x,\mu) \qquad \boldsymbol{F}_\mathrm{b}^\mathrm{H}\boldsymbol{K}(x,\mu) = \boldsymbol{0}, \tag{20}$$

$$\tilde{L}\tilde{\boldsymbol{K}}(x,\mu) = s_\mu^*\boldsymbol{C}^\mathrm{H}\tilde{\boldsymbol{K}}(x,\mu) \qquad \tilde{\boldsymbol{F}}_\mathrm{b}^\mathrm{H}\tilde{\boldsymbol{K}}(x,\mu) = \boldsymbol{0}, \tag{21}$$

with the adjoint differential operator and boundary matrix

$$\tilde{L} = \boldsymbol{A}^{\mathrm{H}} - \boldsymbol{I}\frac{\partial}{\partial x} \qquad \tilde{\boldsymbol{F}}_{\mathrm{b}}^{\mathrm{H}} = \boldsymbol{I} - \boldsymbol{F}_{\mathrm{b}}^{\mathrm{H}}. \tag{22}$$

Indeed, Eq. 16 follows by applying the SLT from (13) to the PDE (2), observing the properties (20) and (21) and integration by parts. From these eigenvalue problems the primal and the adjoint eigenfunctions are calculated, see Sec. 3.6.

3.4. Kernel functions

To calculate the eigenfunctions $\boldsymbol{K}(x,\mu)$ and $\tilde{\boldsymbol{K}}(x,\mu)$ from the eigenvalue problems, Eqs. (20) and (21) are reformulated as

$$\partial_x \boldsymbol{K}(x,\mu) = \boldsymbol{Q}\boldsymbol{K}(x,\mu), \tag{23}$$

$$\partial_x \tilde{\boldsymbol{K}}(x,\mu) = \tilde{\boldsymbol{Q}}\tilde{\boldsymbol{K}}(x,\mu), \tag{24}$$

with

$$\boldsymbol{Q} = s_\mu \boldsymbol{C} - \boldsymbol{A}, \tag{25}$$

$$\tilde{\boldsymbol{Q}} = \boldsymbol{A}^{\mathrm{H}} - s_\mu^* \boldsymbol{C}^{\mathrm{H}} = -\boldsymbol{Q}^{\mathrm{H}}. \tag{26}$$

The solution of the primal eigenvalue problem for the eigenfunctions can be formulated in terms of a matrix exponential

$$\boldsymbol{K}(x,\mu) = e^{\boldsymbol{Q}x}\boldsymbol{K}(0,\mu), \tag{27}$$

where $\boldsymbol{K}(0,\mu)$ is the boundary vector of the eigenfunctions. The matrix exponential can be calculated using the method from [12], or by any other suitable method. The solution for the adjoint kernel function $\tilde{\boldsymbol{K}}(x,\mu)$ is formulated analogously.

3.5. Eigenvalues and Eigenfrequencies

To calculate the kernel functions with Eq. (27) the eigenvalues λ of matrix $\boldsymbol{Q}$ and the eigenfrequencies s_μ of the string model have to be derived. Therefore the characteristic polynomial $p_{\mathrm{Q}}(\lambda)$ of the matrix $\boldsymbol{Q}$ is calculated. It follows from Eq. (25) as

$$p_{\mathrm{Q}}(\lambda) = \lambda^4 - q_2\lambda^2 - q_1 s_\mu, \tag{28}$$

with the coefficients

$$q_1 = c_1 s_\mu - a_1 \qquad q_2 = c_2 s_\mu - a_2. \tag{29}$$

With relation between the eigenvalues

$$\lambda_2 = -\lambda_1 \qquad \lambda_4 = -\lambda_3, \tag{30}$$

follows for the eigenvalues of the matrix $\boldsymbol{Q}$

$$\lambda_{1/3}^2 = \frac{1}{2}\left(q_2 \pm \sqrt{q_2^2 + 4q_1 s_\mu}\right). \tag{31}$$

By evaluating the boundary conditions for the eigenfunctions in Eqs. (23) and (24), it can be shown that the eigenvalues λ can only adopt values of the form

$$\lambda = \lambda_\mu = j\mu\frac{\pi}{l} = j\gamma_\mu. \tag{32}$$

Setting Eq. (28) to zero and solving for the eigenfrequencies s_μ leads to the dispersion relation

$$s_\mu^2 + \left(\frac{a_1}{c_1} - \lambda^2\frac{c_2}{c_1}\right)s_\mu - \frac{\lambda^2}{c_1}\left(\lambda^2 + a_2\right) = 0. \tag{33}$$

The eigenfrequencies s_μ are the solutions of the dispersion relation (33) for λ from (32). For each value of γ_μ the dispersion relation yields two complex conjugate eigenfrequencies s_μ.

3.6. Solution for the kernels

Using the derivations from the previous sections the eigenfunctions can be calculated from Eq. (27). Skipping many explicit calculations, the eigenfunction $\boldsymbol{K}(x,\mu)$ results in

$$\boldsymbol{K}(x,\mu) = \begin{bmatrix} \frac{s_\mu}{\gamma_\mu}\sin(\gamma_\mu x) \\ \cos(\gamma_\mu x) \\ -\gamma_\mu \sin(\gamma_\mu x) \\ -\gamma_\mu^2 \cos(\gamma_\mu x) \end{bmatrix}, \tag{34}$$

and similar for the adjoint eigenfunction function

$$\tilde{\boldsymbol{K}}(x,\mu) = \begin{bmatrix} q_1^* \cos(\gamma_\mu x) \\ -\frac{s_\mu^* q_1^*}{\gamma_\mu}\sin(\gamma_\mu x) \\ -\gamma_\mu^2 \cos(\gamma_\mu x) \\ \gamma_\mu \sin(\gamma_\mu x) \end{bmatrix}. \tag{35}$$

These solutions can be verified via inserting them into the eigenvalue problems from the Eqs. (23) and (24).

3.7. Output Signal

The results from the previous sections can now be used to construct the synthesis equation for the string, which is based on the inverse SLT from Eq. (14). As mentioned in Sec. 3.5 for one μ-value a complex conjugated pair of eigenfrequencies s_μ arises in Eq. (33). Setting the excitation function $f_{\mathrm{e}}(x,t)$ to zero for brevity, the synthesis equation turns into

$$\begin{aligned} \boldsymbol{Y}(x,s) &= \sum_\mu \frac{1}{N_\mu}\boldsymbol{K}(x,\mu)\bar{Y}(\mu,s) = \\ &= \sum_\mu \frac{1}{N_\mu}\boldsymbol{K}(x,\mu)\frac{1}{s-s_\mu}\bar{\Phi}(\mu,s). \end{aligned} \tag{36}$$

The resulting synthesis system is pictured in Fig. 1. The output $\boldsymbol{Y}(x,s)$ is a superposition of many first-order systems – oscillating with the eigenfrequencies of the system and weighted with the eigenfunctions $\boldsymbol{K}(x,\mu)$. For a more suitable implementation, each pair of complex conjugate first-order systems may be merged into one real-valued second-order system.

3.8. Discrete-time equivalent

This synthesis structure can be transformed into the discrete-time domain to achieve a difference equation for computer implementation. Using e.g. impulse-invariant-transformation [6] turns the transfer function from Eq. (19) into

$$\bar{Y}(\mu,z) = \frac{z}{z-z_\mu}\bar{\Phi}(\mu,z), \tag{37}$$

where $\bar{Y}(\mu,z)$ and $\bar{\Phi}(\mu,z)$ are the z-domain equivalents of $\bar{Y}(\mu,s)$ and $\bar{\Phi}(\mu,s)$. The poles z_μ are defined as

$$z_\mu = \exp\left(s_\mu T\right), \tag{38}$$

with the sampling time T.

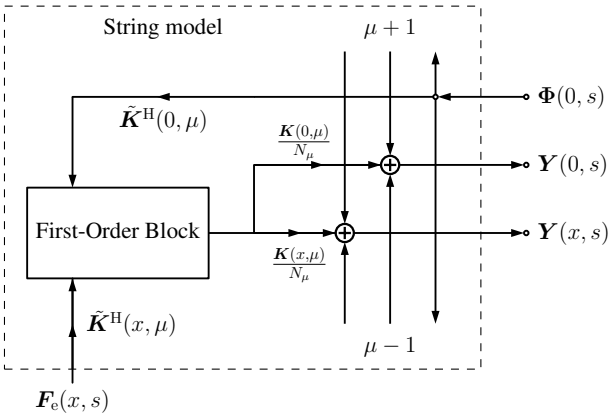

Figure 1: Block diagram of the synthesis system; $\boldsymbol{\Phi}(0,s)$, $\boldsymbol{Y}(0,s)$: Vector of boundary excitations/observations at $x=0$, $\boldsymbol{Y}(x,s)$: vector of output signals at any position x, $\boldsymbol{F}_{\mathrm{e}}(x,s)$: Excitation function.

4. ADJUSTABLE BOUNDARY CONDITIONS

The boundary conditions of a PDE are essential for the transformation with the FTM, but the more complex the boundary conditions are, the more complex becomes the transformation. Using adjustable boundary conditions means to transform the PDE including a simple set of boundary conditions and later adjust them to fulfill any kind of boundary condition [8, 9].

4.1. Simple Boundary Conditions

As starting point, the simple set of boundary conditions from Sec. 2.2 are revisited. The boundary behavior at $x=0$ as described by Eqs. (8) and (9) in terms of the boundary matrix $\boldsymbol{F}_{\mathrm{b}}^{\mathrm{H}}$ and a vector of boundary excitations $\boldsymbol{\Phi}(0,s)$ reads in the frequency domain

$$\boldsymbol{F}_{\mathrm{b}}^{\mathrm{H}}\boldsymbol{Y}(0,s)=\begin{bmatrix}1&0&0&0\\0&0&0&0\\0&0&1&0\\0&0&0&0\end{bmatrix}\begin{bmatrix}sY(0,s)\\Y'(0,s)\\Y''(0,s)\\Y'''(0,s)\end{bmatrix}=\begin{bmatrix}\dot{\Phi}_1\\0\\\Phi_3\\0\end{bmatrix}. \quad (39)$$

In addition an observation matrix $\boldsymbol{F}_{\mathrm{o}}^{\mathrm{H}}$ is defined. It transforms the vector of variables $\boldsymbol{Y}(x,s)$ into a vector of boundary observations $\boldsymbol{Y}_{\mathrm{o}}$, which can be written as

$$\boldsymbol{F}_{\mathrm{o}}^{\mathrm{H}}\boldsymbol{Y}(0,s)=\begin{bmatrix}0&0&0&0\\0&1&0&0\\0&0&0&0\\0&0&0&1\end{bmatrix}\begin{bmatrix}sY(0,s)\\Y'(0,s)\\Y''(0,s)\\Y'''(0,s)\end{bmatrix}=\begin{bmatrix}0\\Y_{\mathrm{o2}}\\0\\Y_{\mathrm{o4}}\end{bmatrix}. \quad (40)$$

The boundary behavior of the variables of the string model can be formulated in terms of the boundary and the observation matrix

$$\boldsymbol{Y}(0,s)=\left(\boldsymbol{F}_{\mathrm{b}}^{\mathrm{H}}+\boldsymbol{F}_{\mathrm{o}}^{\mathrm{H}}\right)\boldsymbol{Y}(0,s), \quad (41)$$

and is pictured at the position $x=0$ in Fig. 2. It shows that the boundary excitations Φ can be interpreted as input variables and the boundary observations as output variables at the boundary of the string.

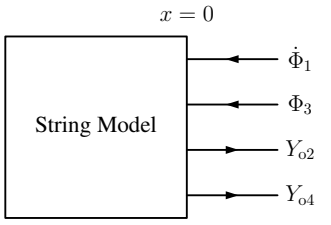

Figure 2: Schematic of the boundary behavior of the string model referring to Eqs. (39) - (40). Y_{o}: Boundary Observations, Φ: Boundary Excitations.

4.2. Impedance Boundary Conditions

In this section, impedance boundary conditions at $x=0$ are investigated (see e.g. [6]). They connect the velocity of the string ($\dot{y}(0,t)$) at the boundary to a force $f(0,t)$ via the mechanical impedance Z_{s} [13]. The force can be exerted e.g. by pressing the ball of the thumb on the bridge to damp the string vibration.

The relation between force and velocity can be formulated in the frequency domain with the Laplace transforms of the velocity $sY(0,s)$ and of the force $F(0,s)$ with the admittance $Y_{\mathrm{s}}=Z_{\mathrm{s}}^{-1}$

$$sY(0,s)-Y_{\mathrm{s}}\,F(0,s)=\Phi_{\mathrm{Z1}}, \quad (42)$$

$$Y''(0,s)=\Phi_{\mathrm{Z3}}, \quad (43)$$

Φ_{Z1} and Φ_{Z3} are the boundary excitations. The force F can be written in the terms of the variables in Eq. (4)

$$F(0,s)=T_{\mathrm{s}}\,Y'(0,s)-EI\,Y''(0,s). \quad (44)$$

The boundary conditions from Eqs. (42) – (43) are rearranged into a boundary matrix, which transforms the variable vector into a vector of boundary excitations

$$\boldsymbol{F}_{\mathrm{bZ}}^{\mathrm{H}}\boldsymbol{Y}(0,s)=\boldsymbol{\Phi}_{\mathrm{Z}}, \quad (45)$$

with

$$\boldsymbol{F}_{\mathrm{bZ}}^{\mathrm{H}}=\begin{bmatrix}1&-Y_{\mathrm{s}}T_{\mathrm{s}}&0&Y_{\mathrm{s}}EI\\0&0&0&0\\0&0&1&0\\0&0&0&0\end{bmatrix}. \quad (46)$$

4.3. Adjustable Boundary Conditions

Using different sets of boundary conditions would mean to recalculate the eigenfunctions from Eqs. (20) and (21) with different boundary conditions and to re-apply the corresponding transformations according to Sec. 3. Furthermore, the determination of the eigenfunctions for impedance boundary conditions does in general not lead to closed form solutions.

A different approach is to use the eigenfunctions for simple boundary conditions from Eqs. (34) and (35) and to feed the boundary observations $\boldsymbol{Y}_{\mathrm{o}}$ from (40) back into the boundary excitations $\dot{\Phi}_1$ and Φ_3 from (39) via the impedance condition (45). This approach had been discussed in general terms in [9] and is now applied to string vibrations.

Starting point is Eq. (45), which can be reformulated using Eq. (41) as

$$\begin{aligned}\boldsymbol{F}_{\mathrm{bZ}}^{\mathrm{H}}\boldsymbol{Y}(0,s) &= \boldsymbol{F}_{\mathrm{bZ}}^{\mathrm{H}}\left(\boldsymbol{F}_{\mathrm{b}}^{\mathrm{H}}+\boldsymbol{F}_{\mathrm{o}}^{\mathrm{H}}\right)\boldsymbol{Y}(0,s)\\ &= \boldsymbol{F}_{\mathrm{bZ}}^{\mathrm{H}}\boldsymbol{F}_{\mathrm{b}}^{\mathrm{H}}\boldsymbol{Y}(0,s)+\boldsymbol{F}_{\mathrm{bZ}}^{\mathrm{H}}\boldsymbol{F}_{\mathrm{o}}^{\mathrm{H}}\boldsymbol{Y}(0,s)=\boldsymbol{\Phi}_{\mathrm{Z}}. \quad (47)\end{aligned}$$

With Eqs. (39) - (40) follows

$$\boldsymbol{F}_{\mathrm{bZ}}^{\mathrm{H}}\boldsymbol{\Phi}=-\boldsymbol{F}_{\mathrm{bZ}}^{\mathrm{H}}\boldsymbol{Y}_{\mathrm{o}}+\boldsymbol{\Phi}_{\mathrm{Z}}. \quad (48)$$

This equation leads to a rule for the transformation of the simple boundary excitations $\boldsymbol{\Phi}$ from Eq. (39) into impedance boundary conditions

$$\begin{bmatrix}\dot{\Phi}_1\\ \Phi_3\end{bmatrix}=Y_{\mathrm{s}}\begin{bmatrix}T_{\mathrm{s}} & -EI\\ 0 & 0\end{bmatrix}\begin{bmatrix}Y_{\mathrm{o}2}\\ Y_{\mathrm{o}4}\end{bmatrix}+\begin{bmatrix}\Phi_{\mathrm{Z}1}\\ \Phi_{\mathrm{Z}3}\end{bmatrix}. \quad (49)$$

The boundary behavior of the string model at $x=0$ is pictured in Fig. 3. It can be seen that the impedance boundary conditions result in a boundary circuit, which adjusts the simple boundary values to fulfill the impedance conditions, according to the transformation rule (49).

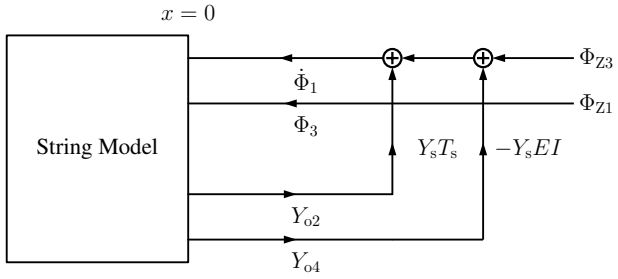

Figure 3: Schematic of the boundary behavior of the string model referring to Eq. (49). Y_{o}: Boundary observations, Φ: Boundary excitations.

With the adjustment of the boundary conditions, one can use a simple model of the string and later adjust the boundaries to match a more complex set of conditions. The adjustment is realized by an external feedback loop between the boundary observations $\boldsymbol{Y}_{\mathrm{o}}$ and the boundary excitations $\dot{\Phi}_1$ and Φ_3.

4.4. Input-Output model for the boundary

This section explains how the output of the string model from Eq. (36) is connected to the boundary circuit from Eq. (49). For the position $x=0$ follows for the eigenfunctions

$$\boldsymbol{K}(0,\mu)=\begin{bmatrix}0 & 1 & 0 & -\gamma_\mu^2\end{bmatrix}^{\mathrm{T}}, \quad (50)$$

$$\tilde{\boldsymbol{K}}^{\mathrm{H}}(0,\mu)=\begin{bmatrix}q_1 & 0 & -\gamma_\mu^2 & 0\end{bmatrix}. \quad (51)$$

Therefore the two non-zero output values of Eq. (41) follow from the z-domain equivalent of (36) as

$$\boldsymbol{Y}_{\mathrm{o}}(z)=\begin{bmatrix}Y_{\mathrm{o}2}(z)\\ Y_{\mathrm{o}4}(z)\end{bmatrix}=\sum_\mu \frac{1}{N_\mu}\bar{Y}(\mu,z)\begin{bmatrix}1\\ -\gamma_\mu^2\end{bmatrix}, \quad (52)$$

where $\bar{Y}(\mu,z)$ is connected to $\bar{\Phi}(\mu,z)$ via Eq. (37).

The boundary term $\bar{\Phi}(\mu,z)$ depends on the boundary conditions $\boldsymbol{\Phi}(0,z)$ and $\boldsymbol{\Phi}(l,z)$ similarly to the continuous-time formulation in (17). Assuming at $x=l$ simple and homogeneous boundary conditions, i.e. $\boldsymbol{\Phi}(l,z)=0$ and at $x=0$ adjustable boundary conditions according to Eq. (49) with $\Phi_3=0$ leaves only a dependency on $\dot{\Phi}_1$. Then $\bar{\Phi}(\mu,z)$ can be expressed using (51) as

$$\bar{\Phi}(\mu,z)=-\bar{\boldsymbol{K}}^{\mathrm{H}}(x,\mu)\boldsymbol{\Phi}(0,z)=-q_1\dot{\Phi}_1(0,z). \quad (53)$$

Now an input-output model for the quantities shown in Fig. 3 can be set up by combining (37) and (52)

$$z\bar{Y}(\mu,z)=z_\mu\bar{Y}(\mu,z)-q_1 z\dot{\Phi}_1(0,z), \quad (54)$$

to obtain the internal variable $\bar{Y}(\mu,z)$ from the boundary input Φ_1 and by using (52) to obtain the boundary output $\boldsymbol{Y}_{\mathrm{o}}$ from $\bar{Y}(\mu,z)$.

However, following the signal flow in (49), (54) and (52) unveils the existence of a delay-free loop. The next section describes how this delay-free loop can be avoided.

5. STATE SPACE MODEL

As described before the adjustment of the boundary conditions according to Eq. (49) causes a delay-free loop in the system. Delay-free loops can be resolved using iterative methods described in [14, 15]. In this paper the delay-free loop is avoided altogether by transformation into a state space model.

5.1. State Equations

At first a state equation is established with the definition of the state variable

$$\bar{W}(\mu,z)=\bar{Y}(\mu,z)+q_1\dot{\Phi}_1(0,z). \quad (55)$$

Since the excitation function $f_{\mathrm{e}}(x,t)$ does not contribute to the boundary feedback and thus to a possible delay-free loop, it is set to zero for brevity.

Rewriting (54) and (52) with the state variable $\bar{W}(\mu,z)$ and collecting the terms depending on μ into vectors and matrices gives finally

$$z\bar{\boldsymbol{W}}(z)=\boldsymbol{A}\bar{\boldsymbol{W}}(z)+\boldsymbol{b}\,\dot{\Phi}_1(0,z), \quad (56)$$

$$\boldsymbol{Y}_{\mathrm{o}}(z)=\boldsymbol{C}_{\mathrm{o}}\bar{\boldsymbol{W}}(z)+\boldsymbol{d}_{\mathrm{o}}\dot{\Phi}_1(0,z). \quad (57)$$

The state and output vectors are given as

$$\bar{\boldsymbol{W}}(z)=\begin{bmatrix}\vdots\\ \bar{W}(\mu,z)\\ \vdots\end{bmatrix}, \qquad \boldsymbol{Y}_{\mathrm{o}}(z)=\begin{bmatrix}Y_{\mathrm{o}2}\\ Y_{\mathrm{o}4}\end{bmatrix}, \quad (58)$$

and the state matrices follow as

$$\boldsymbol{A}=\mathrm{diag}\left(\dots,z_\mu,\dots\right), \quad (59)$$

$$\boldsymbol{b}=\left[\dots,z_\mu q_1(s_\mu),\dots\right], \quad (60)$$

$$\boldsymbol{C}_{\mathrm{o}}=\left[\dots,\frac{1}{N_\mu}\begin{bmatrix}1\\ -\gamma_\mu^2\end{bmatrix},\dots\right], \quad (61)$$

$$\boldsymbol{d}_{\mathrm{o}}=\sum_\mu\frac{q_1(s_\mu)}{N_\mu}\begin{bmatrix}1\\ -\gamma_\mu^2\end{bmatrix}. \quad (62)$$

5.2. Feedback Loop

To fit the boundary behavior in Fig. 3 into the state space equations (56) - (57), the boundary equation (49) is reformulated (with $\Phi_{\mathrm{Z1}} = \Phi_{\mathrm{Z3}} = 0$) as

$$\dot{\Phi}_1(0,z) = Y_\mathrm{s}\, \boldsymbol{r}^\mathrm{T} \boldsymbol{Y}_\mathrm{o}(z), \tag{63}$$

with the vector

$$\boldsymbol{r}^\mathrm{T} = [T_s \; -EI]\,. \tag{64}$$

It is part of a delay-free loop, where the remaining part is formed by the direct path in (57).

To avoid this delay-free loop, Eq. (63) is inserted into (57) and solved for the output vector $\boldsymbol{Y}_\mathrm{o}(z)$

$$\boldsymbol{Y}_\mathrm{o}(z) = \left(\boldsymbol{I} - Y_\mathrm{s}\, \boldsymbol{d}_\mathrm{o} \boldsymbol{r}^\mathrm{T}\right)^{-1} \boldsymbol{C}_\mathrm{o} \bar{\boldsymbol{W}}(z). \tag{65}$$

Now the boundary input can be expressed directly in terms of the state vector $\bar{\boldsymbol{W}}(z)$ with the help of (63) and (65)

$$\dot{\Phi}_1(0,z) = Y_\mathrm{s} \boldsymbol{r}^\mathrm{T} \left(\boldsymbol{I} - Y_\mathrm{s} \boldsymbol{d}_\mathrm{o} \boldsymbol{r}^\mathrm{T}\right)^{-1} \boldsymbol{C}_\mathrm{o} \bar{\boldsymbol{W}}(z) = \boldsymbol{r}_\mathrm{b}^\mathrm{T} \bar{\boldsymbol{W}}(z). \tag{66}$$

The vector $\boldsymbol{r}_\mathrm{b}$ contains the influence of the admittance Y_s at the boundary and can be reformulated using the Sherman-Morisson identity [16, eq. (160)]

$$\boldsymbol{r}_\mathrm{b}^\mathrm{T} = Y_\mathrm{s} \boldsymbol{r}^\mathrm{T} \left(\boldsymbol{I} - Y_\mathrm{s} \boldsymbol{d}_\mathrm{o} \boldsymbol{r}^\mathrm{T}\right)^{-1} \boldsymbol{C}_\mathrm{o} = \frac{1}{Z_\mathrm{s} - \boldsymbol{r}^\mathrm{T} \boldsymbol{d}_\mathrm{o}} \boldsymbol{r}^\mathrm{T} \boldsymbol{C}_\mathrm{o}. \tag{67}$$

5.3. Simulation Model

The final simulation model for adjustable boundary conditions follows from the state space representation (56) and (57) and the description of the outer feedback loop by (66). The structure of the model is shown in Fig. 4.

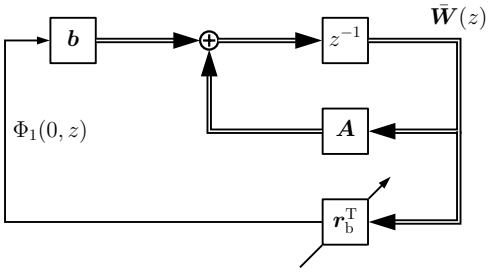

Figure 4: Signal flow of the state space equations from (56) and (57) including the boundary feedback loop of Eq. (66).

There are two loops and both include a time delay z^{-1}. The inner loop is closed by the diagonal matrix $\boldsymbol{A}$ from Eq. (59) and is easy to implement. The outer loop contains the boundary admittance Y_s or impedance Z_s according to (63). So the delay-free loop arising in Sec. 4.4 is avoided using the state space structure. The output-equation (57) calculates the output of the model for the position $x = 0$ (Feedback path in Fig. 4).

The output signal at any other position $x = x_\mathrm{a}$ on the string is calculated by a second output equation

$$\boldsymbol{Y}_\mathrm{a}(z) = \boldsymbol{C}_\mathrm{a} \bar{\boldsymbol{W}}(z) + \boldsymbol{d}_\mathrm{a} \dot{\Phi}_1(0,z), \tag{68}$$

which is basically the same as for $x = 0$. Only two matrices and vectors have to be recalculated

$$\boldsymbol{C}_\mathrm{a} = \left[\ldots, \frac{1}{N_\mu} \boldsymbol{K}(x_\mathrm{a}, \mu), \ldots\right], \tag{69}$$

$$\boldsymbol{d}_\mathrm{a} = \sum_\mu \frac{q_1(s_\mu)}{N_\mu} \boldsymbol{K}(x_\mathrm{a}, \mu). \tag{70}$$

The other matrices are independent of the pick-up position x_a, so they can be directly taken from Eqs. (59) - (60). The complexity of the feedback loop at the position $x = 0$ is hidden in the vector $\boldsymbol{r}_\mathrm{b}^\mathrm{T}$, which is independent of any pick-up point on the string. Thus the feedback path is variable by adjusting the value for the impedance Z_s in (67), see Fig. 4.

6. EXAMPLES

The following section presents simulation results, which are based on the theory from previous sections. The simulation uses the string model from Sec. 3 with a simple set of boundary conditions, which are adjusted to fulfill the impedance boundary conditions using the concept from Sec. 4.3. The model is implemented with the state space representation from Sec. 5 to avoid delay-free loops.

6.1. Basic Parameters

The string model for the simulation is based on the transformation of the PDE of a vibrating string and the subsequent state space representation from Eqs. (56) - (57). The boundary conditions of the string are pictured in Fig. 5. The string has a supported end at $x = l$, which results in homogeneous boundary conditions referring to (7)

$$Y(x,s) = 0, \qquad Y''(x,s) = 0 \qquad x = l. \tag{71}$$

At the position $x = 0$ the string is placed on the bridge and is influenced by an admittance, which results in impedance boundary conditions from Eqs. (42) - (43). The boundary excitations Φ_{Z1} and Φ_{Z3} are set to zero since there are no external forces. The mechanical admittance Y_s is used as an adjustable parameter and is considered as frequency independent.

For the simulations a nylon guitar B string was used. The physical parameters of the string are taken from [6, 17] and are listed in Table 1.

ρ	Density	$1140\,\mathrm{kg/m^3}$
E	Young's modulus	$5.4\,\mathrm{GPa}$
l	Length	$0.65\,\mathrm{m}$
A	Cross section area	$0.5188\,\mathrm{mm^2}$
I	Moment of inertia	$0.141\,\mathrm{mm^4}$
d_1	Freq. indep. damping	$8 \cdot 10^{-5}\,\mathrm{kg/(ms)}$
d_3	Freq. dep. damping	$-1.4 \cdot 10^{-5}\,\mathrm{kgm/s}$
T_S	Tension	$60.97\,\mathrm{N}$

Table 1: Physical parameters of a nylon guitar B string.

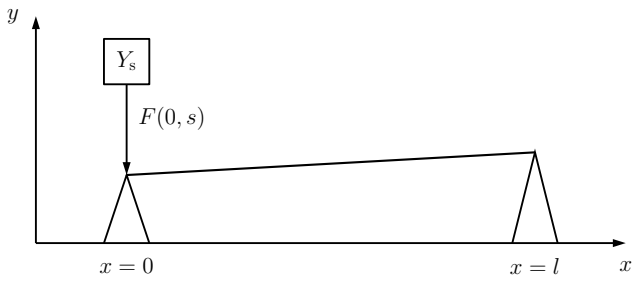

Figure 5: Guitar string influenced by an impedance/admittance caused e.g. the ball of players hand at bridge position $x = 0$ and a supported end at $x = l$.

6.2. Simulation Results

The following section presents the results of the simulation of the string model based on the previous chapters. At first, the influence of the admittance Y_s on the bending $y'(0,t)$ at the position $x = 0$ is shown. Then the influence on the velocity $\dot{y}(x_\mathrm{a},t)$ at a specific pick-up point $x = x_\mathrm{a}$ is presented. In each case the signal is pictured for three admittance values between $Y_\mathrm{s} = 0$ and $Y_\mathrm{s} = 0.125\,\frac{\mathrm{s}}{\mathrm{kg}}$. The string is excited by a single impulse at the position $x_\mathrm{e} = 0.5\,\mathrm{m}$

$$f_\mathrm{e}(x) = \begin{cases} 50\,\mathrm{mN} & x = x_\mathrm{e} \\ 0 & x \neq x_\mathrm{e} \end{cases}. \tag{72}$$

The results are presented by the normalized amplitude spectra of the velocity and bending. At first results for a zero admittance ($Y_\mathrm{s} = 0$) are presented, then the admittance is varied and also a non-zero pick-up position is considered.

Results for zero admittance

In this part the string model from Eq. (36) using $\mu = 1 \ldots 100$ complex eigenfrequencies with the simple set of boundary conditions from Sec. 4.1 is considered. For the implementation the state space representations from Eqs. (56) - (57) is used with $\Phi_1 = 0$. Fig. 6 shows the variation of the bending $y'(x,t)$ over time and pick-up position for a mechanical admittance $Y_\mathrm{s} = 0\,\mathrm{s/kg}$.

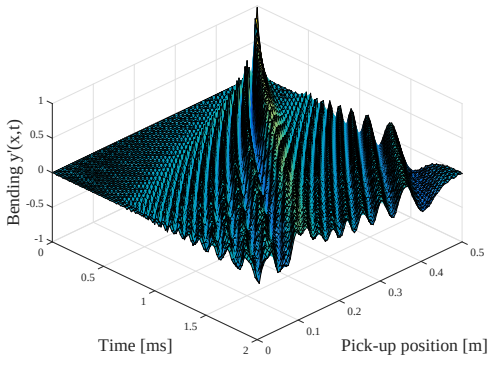

Figure 6: Variation of the bending $y'(x,t)$ over time at different pick-up positions on the string for $Y_\mathrm{s} = 0\,\mathrm{s/kg}$.

The excitation function in Fig. 6 is an impulse according to Eq. (72). It causes the propagation of waves on the string. The results show that the derived string model matches the behavior of a real string for simple boundary conditions [6–8, 10].

Results for non-zero admittance

The following experiments show the behavior of the spring model using the impedance boundary conditions from Sec. 4.2. The implementation uses the state space representation from Eqs. (56) - (57), with boundary term $\dot{\Phi}_1$ from Eq. (66). The admittance is varied between $Y_\mathrm{s} = 0$ and a maximum value of $Y_\mathrm{s} = 0.125\,\mathrm{s/kg}$, which is taken from [7].

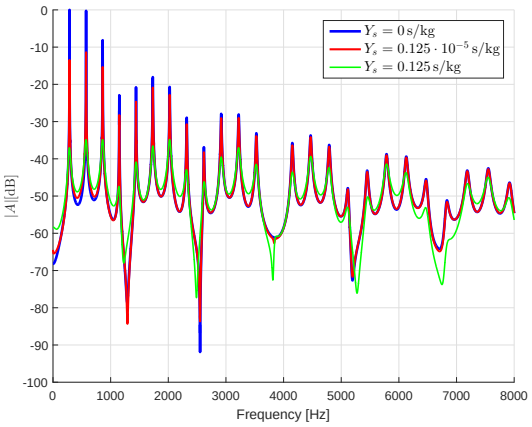

Figure 7: Amplitude spectra of bending $y'(x,t)$ at the bridge position $x = 0$.

Fig. 7 shows the amplitude spectra of bending $y'(x,t)$ at the position $x = 0$ for different admittance values. For an admittance value of $Y_\mathrm{s} = 0$ results the spectrum of a string with simple boundary conditions, as the lower feedback path in Fig. 4 is zero. For an admittance value $Y_\mathrm{s} = 0.125 \cdot 10^{-5}\,\mathrm{s/kg}$ the damping influence of the admittance on the bending can be seen clearly, especially in the low-frequency region. For the maximum value of admittance $Y_\mathrm{s} = 0.125\,\mathrm{s/kg}$ the whole spectrum is damped and is much flatter. Thus the increase of the admittance value leads to the well known effect of a decreased oscillation time of the system. This reproduces the sound of a palm muted playing style.

With the increasing value of mechanical admittance, the poles z_μ of the simple string model are shifted towards the origin of the unit circle by the impedance boundary condition feedback loop. Thus the Euclidean distance of the poles is reduced and the single frequency components of the signal are damped depending on the value of the admittance.

Fig. 8 shows the spectra of velocity $\dot{y}(x,t)$ at the pick-up position $x_\mathrm{a} = 0.4\,\mathrm{m}$ for the same three values of admittance Y_s. The general behavior of the spectra is similar to the behavior in Fig. 7. But especially the influence of the feedback loop for the mid-value of Y_s is not so strong at $x = 0.4\,\mathrm{m}$ as for $x = 0$ in Fig. 7. This makes sense, as the pick-up point is removed by $x = 0.4\,\mathrm{m}$ from the bridge position of the guitar, so the damping influence is not as strong as for the bridge position. For the maximum value of the admittance, the spectrum is similarly flat as before at the position $x = 0$.

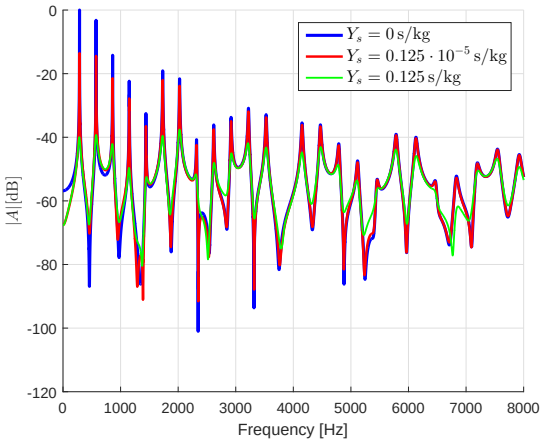

Figure 8: Amplitude spectra of velocity $\dot{y}(x,t)$ at the position $x = 0.4\,\mathrm{m}$.

For both pick-up positions the influence of the admittance damps the harmonics of the output signal. According to different values of the admittance, the signals sounds fully or partially muted.

7. CONCLUSIONS AND FURTHER WORK

This paper proposes a complex string model with general boundary conditions. It is realized by standard state space methods based on the functional transformation method. Then the simple boundary conditions for supported ends are adjusted to impedance boundary conditions, without the need for a recalculation of the eigenfunctions. Using this principle, the simple string model is connected to an admittance at the bridge position.

Here a frequency independent admittance is adopted. It is suitable for modeling a palm muted playing style where the ball of the players hand damps the strings. Other types of boundary conditions require frequency dependent admittances. For example it is well known that the connection of a string to a sound board exhibits strong resonances [17]. They are described by a bridge impedance with multiple poles [4]. Frequency dependent impedances of this type can be modeled with an arrangement similar to Fig. 4, where the feedback path includes a digital filter with complex poles. Another way is to exploit the parallel resonator structure of the functional transformation method by merging the impedance feedback path with the $\boldsymbol{A}$ matrix of the state space representation. Then each diagonal entry of the matrix $\boldsymbol{A}$ can be weighted by a different impedance value as proposed in [8].

8. REFERENCES

[1] Neville H. Fletcher and Thomas D. Rossing, *The Physics of Musical Instruments*, Springer-Verlag, New York, USA, 2nd edition, 1998.

[2] Stefan Bilbao, *Numerical Sound Synthesis*, John Wiley and Sons, Chichester, UK, 2009.

[3] V. Välimäki, J. Pakarinen, C. Erkut, and M. Karjalainen, "Discrete time modeling of musical instruments," *Reports on Progress in Physics*, vol. 69, pp. 1–78, 2006.

[4] Julius O. Smith III, *Physical Audio Signal Processing*, W3K Publishing, 2010, http://www.w3k.org/books.

[5] Cumhur Erkut, *Aspects in Analysis and Model-based Sound Synthesis of Plucked String Instruments*, Ph.D. thesis, Helsinki University of Technology, Espoo, Finland, 2002.

[6] R. Rabenstein and L. Trautmann, "Digital sound synthesis of string instruments with the functional transformation method," *Signal Processing*, vol. 83, no. 8, pp. 1673–1688, August 2003.

[7] Lutz Trautmann and Rudolf Rabenstein, *Digital Sound Synthesis by Physical Modeling using the Functional Transformation Method*, Kluwer Academic Publishers, New York, USA, 2003.

[8] L. Trautmann, S. Petrausch, and M. Bauer, "Simulations of string vibrations with boundary conditions of third kind using the functional transformation method," *The Journal of the Acoustical Society of America (JASA)*, vol. 118, no. 3, pp. 1763–1775, September 2005.

[9] R. Rabenstein and S. Petrausch, "Adjustable boundary conditions for multidimensional transfer function models," in *10th International Conference on Digital Audio Effects (DAFx-07)*, Bordeaux, France, September 2007, pp. 305–310.

[10] S. Petrausch and R. Rabenstein, "A simplified design of multidimensional transfer function models," in *International Workshop on Spectral Methods and Multirate Signal Processing (SMMSP2004)*, Vienna, Austria, September 2004, pp. 35–40.

[11] Julien Bensa, Stefan Bilbao, Richard Kronland-Martinet, and Julius O. Smith, "The simulation of piano string vibration: From physical models to finite difference schemes and digital waveguides," *The Journal of the Acoustical Society of America*, vol. 114, no. 2, pp. 1095–1107, 2003.

[12] U. Luther and K. Rost, "Matrix Exponentials and Inversion of Confluent Vandermonde Matrices," *Electronic Transactions on Numerical Analysis*, vol. 18, pp. 91–100, 2004.

[13] A.D. Pierce, *Acoustics – An Introduction to its physical principles and applications*, Acoustical Society of America, 1991, reprint.

[14] A. Härmä, "Implementation of recursive filters having delay free loops," *1998. Proceedings of the 1998 IEEE International Conference on Acoustics, Speech and Signal Processing*, vol. 3, pp. 1261–1264, May 1998.

[15] G. Borin, G. De Poli, and D. Rocchesso, "Elimination of delay-free loops in discrete-time models of nonlinear acoustic systems," *IEEE Transactions on Speech and Audio Processing*, vol. 8, no. 5, pp. 597–605, Sep. 2000.

[16] K. B. Petersen and M. S. Pedersen, "The matrix cookbook," http://www2.imm.dtu.dk/pubdb/p.php?3274, Nov 2012, Version 20121115.

[17] O. Christensen, "An oscillator model for analysis of guitar sound pressure response," *Acta Acustica united with Acustica*, vol. 54, no. 5, pp. 289–295, 1984.